ISIJ International, Vol. 52 (2012), No. 12, pp. 2273–2277

Iron Aluminide Coatings by Electrodeposition of Aluminum from an Organic Bath and Subsequent Annealing

Masao MIYAKE, Hiroshi MOTONAMI and Tetsuji HIRATO*

Graduate School of Energy Science, Kyoto University, Yoshida-honmachi, Sakyo-ku, Kyoto, 606-8501 Japan.

(*Received on July 31, 2012; accepted on August 20, 2012*)

Oxidation-resistant Fe–Al alloy coatings were formed on Fe substrate by a process using electrodeposition of Al and annealing. Electrodeposition in a dimethylsulfone-aluminum chloride bath containing an additive at 110°C yielded a dense Al layer adherent to the Fe substrate. Annealing of the Fe substrate with the electrodeposited Al layer generated an Fe_2Al_5 layer on the surface at 700°C and 800°C, and an FeAl layer at 900°C through interdiffusion. Oxidation tests at 600°C and 800°C confirmed that the FeAl layer formed through the process could act as an oxidation-resistant coating.

KEY WORDS: electroplating; organic solvent; aluminizing; heat treatment; intermetallics.

1. Introduction

Aluminizing is a surface treatment to enhance the oxidation-resistance of steels and iron-based materials for high-temperature applications in oxidizing environments such as boilers and steam turbines.[1)] The treatments generate Fe–Al alloy layers on the surface by reaction diffusion between Al and Fe. As can be expected from the phase diagram of the Fe–Al system (**Fig. 1**),[2)] several alloy phases can be formed by the treatment. The oxidation-resistance of the alloys should increase with increasing Al content, because their oxidation-resistance is based on the capability of forming a dense, protective Al_2O_3 surface layer. The Al-rich intermetallic compounds, $FeAl_3$, Fe_2Al_5 and $FeAl_2$, are, however, brittle and are thus subject to lower plastic formability and thermal stress fractures.[3)] FeAl, which has a relatively high workability and wear resistance, is therefore considered to be the most appropriate phase for an oxidation-resistant coating.[4,5)]

While various processes for the aluminizing have been developed, including hot-dipping,[6,7)] pack cementation,[8)] spray coating[9)] and foil-aluminizing,[5)] we have proposed a new process composed of electrodeposition of Al and subsequent annealing.[10–12)] This approach using electrodeposition has advantages over the aforementioned processes in that an Al layer can be formed even on surfaces with complex shapes at a low cost. Our previous studies demonstrated that aluminide layers can be formed on Ni,[10)] Ti,[11)] and TiAl substrates[12)] by this process.

In this paper, we examine the applicability of this aluminizing process to Fe substrate. Electrodeposition of Al was performed on an Fe substrate from an organic solvent, dimethylsulfone ($DMSO_2$), and annealing was then conducted in the temperature range from 700 to 900°C to elucidate the alloy phase formed on the Fe substrate. The oxidation-resistance of the resulting alloy coating was verified.

2. Experimental Section

Preparation of the electrolytic bath and electrodeposition of Al were carried out in an Ar-filled glove box equipped with a circulation system. $DMSO_2$ (Tokyo Chemical Industry, 99%) and anhydrous $AlCl_3$ grains (Fluka, crystallized, 99%) were used as the solvent and Al source, respectively. Trimethylamine hydrochloride (TMA, Sigma-Aldrich, 99%) was added to the bath as an additive to inhibit the incorporation of impurities such as sulfur and chlorine to the electrodeposited Al layer.[13)] The $DMSO_2$ and TMA were used after drying for 24 h at 60°C and 90°C, respectively, while $AlCl_3$ was used as received. The molar ratio of $DMSO_2$: $AlCl_3$: TMA in the electrolyte was 10 : 2 : 0.2. A glass vessel with a volume of 150 mL was used as the electrochem-

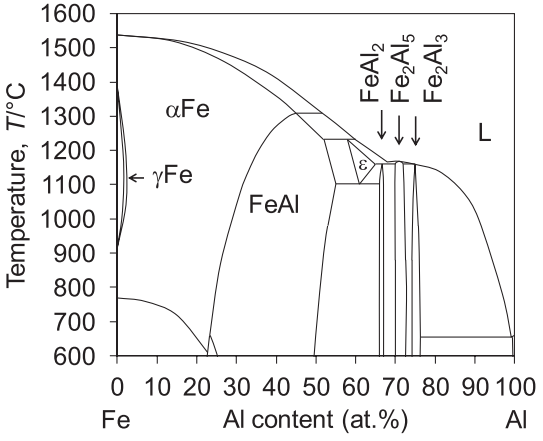

Fig. 1. Phase diagram of the Al–Fe system.[2)]

* Corresponding author: E-mail: hirato.tetsuji.2n@kyoto-u.ac.jp
DOI: http://dx.doi.org/10.2355/isijinternational.52.2273

ical cell. An Fe plate (Nilaco, 99.5%) with a thickness of 1 mm and an Al plate (Nilaco, 99%) were used as the substrate and counter electrode, respectively. A part of the Fe plate was covered with PTFE tape so that only a certain area (10×10 mm^2) would be exposed. Galvanostatic electrodeposition was performed with an electrochemical analyzer (ALS, model 660 C). The temperature of the electrolyte was maintained at 110°C by a thermostat. The electrolyte was stirred by a magnetic stirrer at 100 rpm during the electrodeposition. After the electrodeposition, the Al coating was washed with copious distilled water.

Annealing of the electrodeposited sample was performed in a vacuum (<0.4 Pa) pulled by a diffusion pump for an hour. In order to avoid crack formation or detachment of the electrodeposited layer as a consequence of the rapid temperature-variation, the samples were heated to the annealing temperatures from ambient temperature at the rate of 10°C min^{-1}, and slowly cooled down in the furnace after the annealing. Oxidation tests of the annealed samples were carried out in air with a furnace (Koyo Thermo Systems, KBF848N1).

Samples were examined by X-ray diffraction (XRD, PANalytical, X'pert PRO-MPD) and a scanning electron microscope (SEM, Hitachi S-3500) equipped with an energy dispersive X-ray spectrometer (EDX). XRD was measured from the surface of the sample. For cross-sectional observation by SEM, samples were cut and polished with diamond paste (1 μm).

3. Results and Discussion

3.1. Electrodeposition of Al Layer on Fe Substrate

An Al layer firmly adhering to the Fe substrate could be obtained by performing galvanostatic electrodeposition at 60 mA cm^{-2} for 1 500 s, *i.e.* 90 C cm^{-2} in the $DMSO_2$–$AlCl_3$ bath containing an additive, TMA. A cross-sectional SEM image and composition profile of the sample (**Fig. 2**) showed the formation of a dense Al layer with thickness of 27–30 μm. The current efficiency for the Al electrodeposition can be estimated to be 87–97% from the thickness of the layer. It should be noted that addition of TMA to the bath was required to form the Al layer adhesive to the substrate. Although electrodeposition in the bath without TMA yielded smooth Al layers, the layers frequently delaminated from the Fe substrate during the subsequent annealing. Our previous study revealed that addition of TMA to the bath suppressed the incorporation of impurities, sulfur and chlorine, originating from the bath into the Al deposits, and thereby resulted in softer Al layers.[13] The exclusion of the impurities and the increase in the ductility are inferred to enhance the adhesion of the Al layer to the substrate.

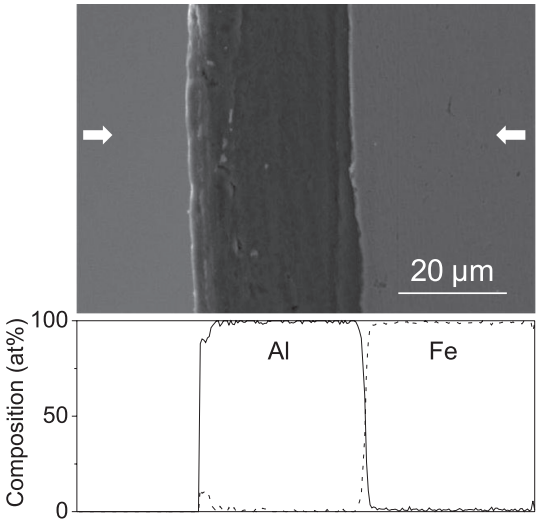

Fig. 2. SEM image and composition profile of cross-section of electrodeposited Al layer on Fe substrate.

3.2. Formation of Alloy Layer by Annealing

The Fe substrate with the electrodeposited Al layer was annealed at 700, 800 and 900°C to form an Fe–Al alloy layer through interdiffusion. **Figures 3–5** show cross-sectional SEM images, composition profiles and XRD patterns of the annealed samples.

The SEM image of the sample annealed at 700°C showed that an alloy layer with an undulating interface was formed in the region from the surface to 30-μm depth (Fig. 3). The composition profile indicated that the Al content of the alloy phase was about 70 at.%, corresponding to the composition of Fe_2Al_5. The XRD pattern taken from the surface of the sample confirmed the formation of the Fe_2Al_5 phase. The high intensity of the Fe_2Al_5 002 diffraction indicates the <001> preferred orientation of the Fe_2Al_5 phase. The growth of the Fe_2Al_5 phase with the <001> preferred orientation is ascribed to the higher diffusion rate in the <001> direction of Fe_2Al_5 phase than in other directions.[14] The pores

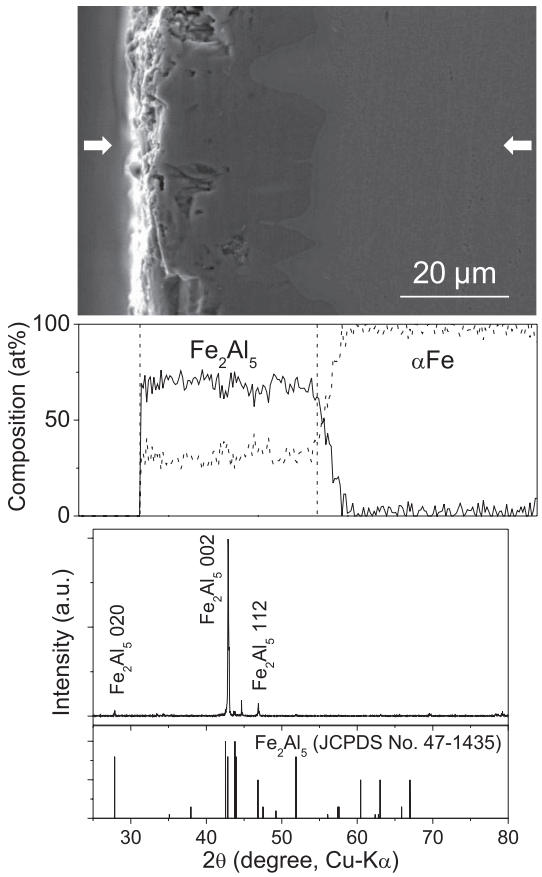

Fig. 3. Cross-sectional SEM image, corresponding composition profile, and XRD pattern taken from surface of sample annealed at 700°C.

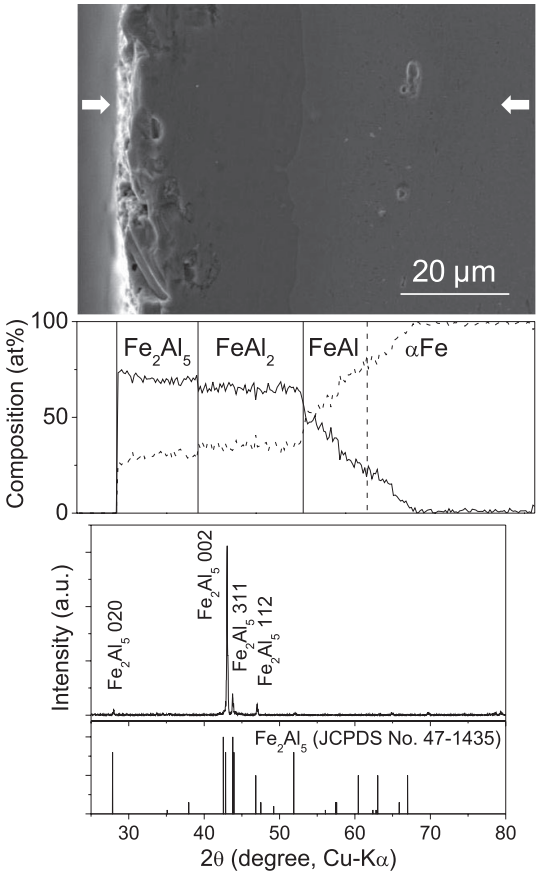

Fig. 4. Cross-sectional SEM image, corresponding composition profile, and XRD pattern taken from surface of sample annealed at 800°C.

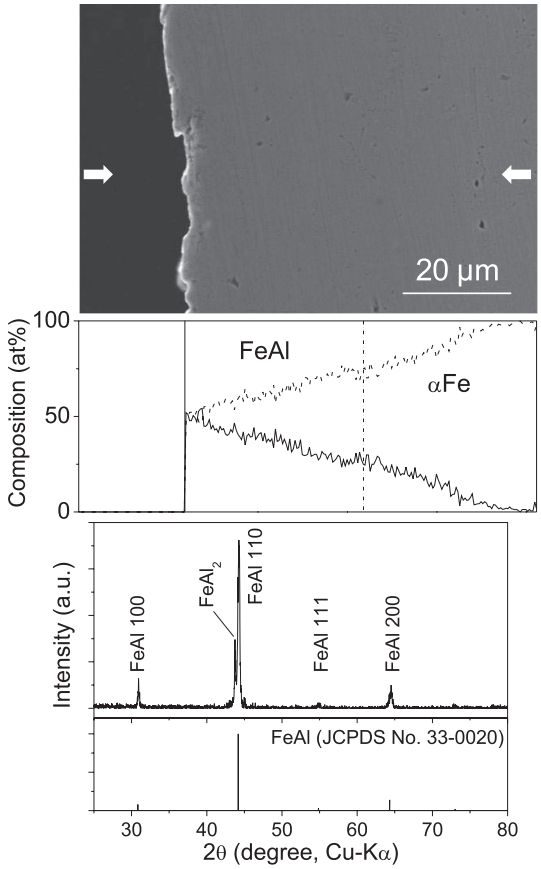

Fig. 5. Cross-sectional SEM image, corresponding composition profile, and XRD pattern taken from surface of sample annealed at 900°C.

observed in the Fe_2Al_5 phase were believed to be formed by the Kirkendall effect.[15)]

In the sample annealed at 800°C, layered alloy phases were observed (Fig. 4). Although the interfaces of the alloy phases were not clear in the SEM image, the composition profile indicated the existence of alloy phases with 70 at.% Al and ~66 at.% Al corresponding to Fe_2Al_5 and $FeAl_2$, respectively. Under the Fe_2Al_5 and $FeAl_2$ layers, there was a region of thickness ~20 μm where the Al content continuously decreased from 50 to 0 at.% with increasing depth. According to the phase diagram (Fig. 1), alloys with the Al content of about 25–50 at.% and 0–25 at.% should be FeAl and αFe phases, respectively. The XRD pattern was almost the same as that of 700°C and in agreement with that of Fe_2Al_5 phase with the <001> preferred orientation. Although the composition profile of the cross-section indicated the formation of $FeAl_2$ phase in addition to Fe_2Al_5, no diffraction peaks from the $FeAl_2$ phase were detected by the XRD, because the $FeAl_2$ phase existed below the thick Fe_2Al_5 layer.

The SEM image of the sample annealed at 900°C showed no clear boundary of alloy layers, but the composition profile indicated that Al diffused into the Fe substrate up to ~55 μm in depth (Fig. 5). The Al content was ~50 at.% near the surface and decreased gradually with increasing depth. According to the phase diagram (Fig. 1), the region from the surface to about 30 μm in depth was inferred to be FeAl phase. Most of the diffraction peaks in the XRD pattern were attributable to those from the FeAl phase. Minor diffraction peaks which could not be ascribed to FeAl were in agreement with those from $FeAl_2$, suggesting that a small amount of $FeAl_2$ was present on the surface although the composition profile could not find the $FeAl_2$ phase. The phase diagram (Fig. 1) suggests a possibility that phase separation occurred from FeAl into FeAl with a smaller Al content and $FeAl_2$ during the cooling process after the annealing at 900°C.

Table 1. Phases formed by annealing at 700, 800 and 900°C.

Temperature, T/°C	Formation phase
700	Fe_2Al_5, αFe
800	Fe_2Al_5, $FeAl_2$, FeAl, αFe
900	$FeAl_2$, FeAl, αFe

Table 1 summarizes the alloy phases formed by the annealing at each temperature. As expected, Fe-richer phases were generated with increasing temperature because the diffusion of Al toward the Fe substrate should proceed more at a higher temperature. While the Fe_2Al_5 layer was generated on the surface of the samples annealed at 700 and 800°C, the FeAl phase, which is considered to be the most appropriate for oxidation-resistance, could be formed as the major phase on the surface by annealing at 900°C. These results are essentially consistent with the cases of the hot-dip and foil aluminizing processes.[5–7)] However, since the thickness of the initial Al layer could be controlled to be thin in the present process, the FeAl layer could be formed in a shorter time.

3.3. Oxidation Test

The Fe substrate, a part of which was coated with the FeAl layer through the process with annealing at 900°C, was heated in air at 600°C for 100 hours to verify the oxidation-resistance of the FeAl coating. In these heating conditions, the bare Fe substrate was heavily oxidized, and a dark-red oxidation product, which easily spalled out, was generated on the surface. Cross-sectional SEM image of the uncoated area revealed that the oxidation layer, which was confirmed to be Fe_2O_3 by XRD analysis, grew up to 80 μm in thickness on the Fe substrate (**Fig. 6**). In contrast, such an oxidation layer was not apparently observed on the surface of the FeAl-coated area. **Figure 7** presents a cross-sectional SEM image, composition profile and XRD pattern of the sample after the oxidation test. Comparison with the data before the oxidation test (Fig. 5) showed no significant change in the morphology and composition profile by the oxidation test, except that the diffusion range of Al was slightly wider. The XRD pattern of the FeAl coating was almost the same before and after the oxidation test; no oxide phase could be detected by XRD even after heating in air for 100 hours. These results demonstrated the high oxidation-resistance of the FeAl coating at 600°C.

The oxidation test was also carried out at a higher temperature, 800°C, in air for 100 hours. In these conditions, the bare Fe substrate with the thickness of 1 mm was completely oxidized. The oxidation product was confirmed to be FeO by XRD in this case. In contrast, XRD analysis of the FeAl-coated area after the oxidation test (**Fig. 8**) showed no distinct diffractions from any oxide phases. The diffraction pattern after the test was attributed to a bcc phase, *i.e.* αFe, indicating that the alloy phase became richer in Fe and thereby changed from FeAl to αFe by the heating. The composition profile of the cross-section clearly showed a decrease in the Al content to less than 20 at.% in most area and a concomitant increase in the thickness of the layer from ~60 μm to ~120 μm, caused by the progress of the interdiffusion at the elevated temperature. The composition profile also indicated the formation of spots with high Al content at the surface and ~30 μm from the surface. The corresponding SEM image showed many voids at the positions with the high Al content. The voids were believed to be formed by the Kirkendall effect.[15] EDX analysis for the

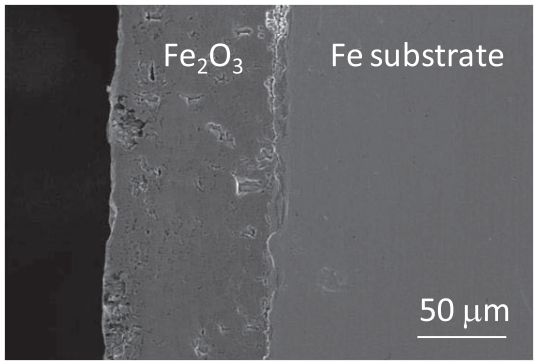

Fig. 6. Cross-sectional SEM image of Fe substrate after oxidation test at 600°C for 100 hours.

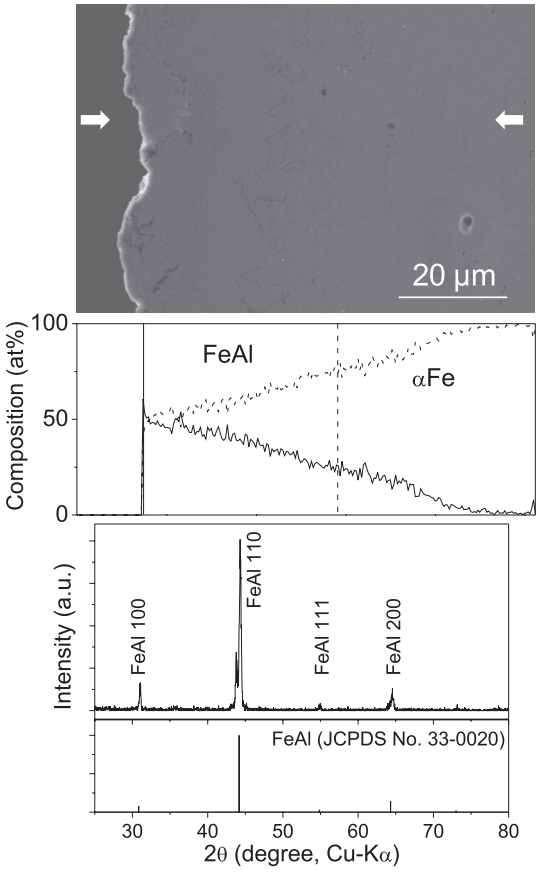

Fig. 7. Cross-sectional SEM image, corresponding composition profile, and XRD pattern taken from surface of TiAl coating after oxidation test 600°C for 100 hours.

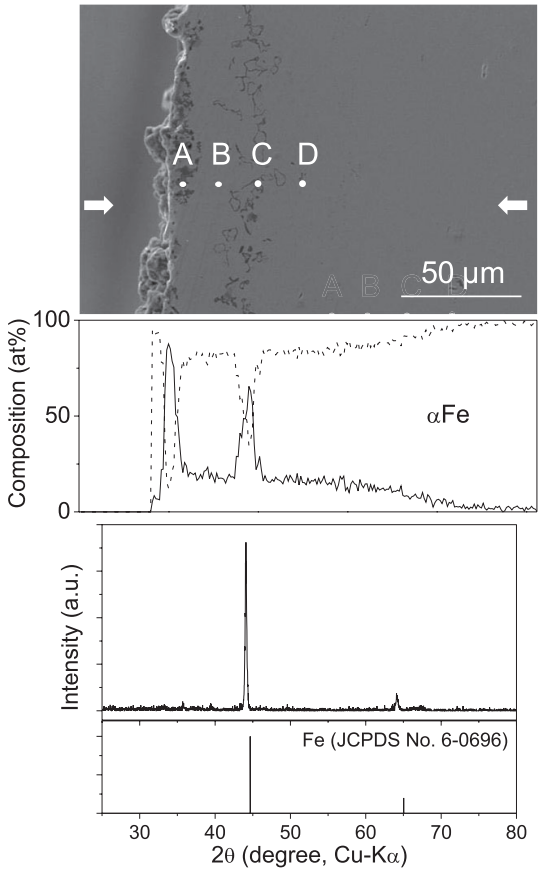

Fig. 8. Cross-sectional SEM image, corresponding composition profile, and XRD pattern taken from surface of TiAl coating after oxidation test 800°C for 100 hours.

Table 2. Composition of the points marked in the SEM image of Fig. 8.

Point	Composition* (at.%)		
	Fe	Al	O
A	15.5	41.5	43.0
B	72.6	19.1	8.3
C	10.5	42.6	46.9
D	77.8	13.0	9.2

*The compositions were determined by EDX, and thus the reliability of the O contents is low.

points marked in the SEM image of Fig. 8 detected high concentrations of Al and O at the voids (**Table 2**), suggesting that the condensation of Al was due to the formation of aluminum oxide at the surface of the voids. Umeda *et al*. also reported the precipitation of aluminum oxide at the Kirkendall voids in foil-aluminizing of a carbon steel.[15] Although a significant change in the composition of the alloy layer occurred, the FeAl coating protected the Fe substrate from oxidation, demonstrating that the FeAl coating can help to extend the lifetime of Fe-based materials even at 800°C.

4. Conclusions

An FeAl oxidation-resistant coating was formed on the Fe substrate by the process using electrodeposition and subsequent annealing. An Al layer firmly adhering to the Fe substrate could be electrodeposited from the $DMSO_2$–$AlCl_3$ bath containing TEA. While annealing of the Fe substrate with the electrodeposited Al layer at 700°C and 800°C yielded an Fe_2Al_5 layer on the surface of the samples, annealing at 900°C generated FeAl as a dominant phase on the surface. The oxidation tests at 600°C and 800°C in air for 100 hours showed that, whereas the bare Fe substrate was heavily oxidized in these conditions, the progress of oxidation into the Fe substrate was not observed in the FeAl-coated area. The FeAl layer formed through the process was demonstrated to work as an oxidation-resistant coating.

Acknowledgment

This work was partly supported by ISIJ Research Promotion Grant.

REFERENCES

1) W. Kai and R. T. Huang: *Oxid. Met.*, **48** (1997), 59.
2) W. Gasior, A. Debski and Z. Moser: *Intermetallics*, **24** (2012), 99.
3) U. Prakash, R. A. Buckley, H. Jones and C. M. Sellars: *ISIJ Int.*, **31** (1991), 1113.
4) T. Skiba, P. Hausild, M. Karlik, K. Vanmeensel and J. Vleugels: *Intermetallics*, **18** (2010), 1410.
5) T. Sasaki and T. Yakou: *Tetsu-to-Hagané*, **89** (2003), 1227.
6) K. Bouche, F. Barbier and A. Coulet: *Mater. Sci. Eng. A*, **249** (1998), 167.
7) S. Kobayashi and T. Yakou: *Mater. Sci. Eng. A*, **338** (2002), 44.
8) C. Houngninou, S. Chevalier and J. P. Larpin: *Appl. Surf. Sci.*, **236** (2004), 256.
9) C.-J. Li, H.-T. Wang, G.-J. Yang and C.-G. Bao: *J. Therm. Spray Technol.*, **20** (2011), 227.
10) S. Shiomi, M. Miyake, T. Hirato and A. Sato: *Mater. Trans.*, **52** (2011), 1216.
11) M. Miyake, S. Tajikara and T. Hirato: *High Temp. Mater. Process.*, **30** (2011), 485.
12) M. Miyake, S. Tajikara and T. Hirato: *Surf. Coat. Technol.*, **205** (2011), 5141.
13) M. Miyake, H. Motonami, S. Shiomi and T. Hirato: *Surf. Coat. Technol.*, **206** (2012), 19.
14) Y. Tanaka and M. Kajihara: *Mater. Trans.*, **50** (2009), 2212.
15) A. Umeda, T. Yakou, K. Kamasaki, N. Nakamura and S.-I. Takagi: *Tetsu-to-Hagané*, **95** (2009), 645.